

Electrochemical Sensor for Ultrasensitive Determination of Atorvastatin Based on Polypyrrole Functionalized Graphene Sheets

Liting Wei*, Haiying Yang, Jiao Jiao

Department of Applied Chemistry, Yuncheng University, Yuncheng, 044000, China;

*E-mail: weiliting_job@163.com

Received: 7 July 2018 / Accepted: 6 September 2018 / Published: 1 October 2018

In this study, polypyrrole functionalized graphene sheets (PPY-GNs) have been used for the first time as a reinforced material for the ultrasensitive detection of atorvastatin by the electrochemistry method. The obtained PPY-GNs were characterized by scanning electron microscopy (SEM) and Fourier transform infrared (FT-IR) spectroscopy. Due to its porous structure, the PPY-GNs-modified electrode has a large effective area, thereby improving the sensitivity of detection. The peak currents of atorvastatin at the GNs-modified glassy carbon electrode (GNs/GCE) and those at the PPY-GNs/GCE are increased dramatically compared to those on the bare GCE. The peak current at the PPY-GNs/GCE linearly increases with the increase in the atorvastatin concentration, which ranges from 20 μ M to 200 μ M. The detection limit of atorvastatin reaches 1.191 μ M based on the signal-to-noise characteristic ($S/N = 3$). The PPY-GNs-based electrochemical sensor was successfully used to detect atorvastatin in tablets with satisfactory results.

Keywords: polypyrrole functionalized graphene sheets; polypyrrole; atorvastatin; electrochemical sensor

1. INTRODUCTION

Atorvastatin, chemically known as (3R,5R)-7-[2-(4-fluorophenyl)-3-phenyl-4-(phenylcarbamoyl)-5-(propan-2-yl)-1H-pyrrol-1-yl]-3,5 dihydroxyheptanoic acid, is used as an anti-inflammatory drug mainly for the treatment of hyperlipidemia and heart disease[1]. Atorvastatin belongs to the statins group, and its structural formula is shown in Fig. 1. In 1985, Bruce D. Roth and Parke-Davis synthesized atorvastatin (ATR), and afterward, it appeared on the market under a variety of brands. Manufacturers use TLC or HPLC to assess the quality of ATR. In addition, various methods have been reported for the drug's determination involving the use of LC/MS [2, 3], HPLC-ES-MS/MS [4] and

various spectrophotometry methods [5-7]. These methods are time-consuming, costly and have low sensitivity. Therefore, it is necessary to develop a rapid and simplified method for the detection of ATR with high sensitivity and low costs. Electrochemical methods with these improved performances could be a great choice. However, the redox reaction of ATR at a bare electrode is generally difficult because of the poor reproducibility and sensitivity. Some functional materials have been synthesized to develop sensitive ATR electrochemical sensors [8, 9].

Graphene, a kind of carbon material, is a two-dimensional carbon lattice composed of sp^2 -bonded carbon atoms; that has attracted widespread attention since its discovery in 2004 [10]. Because of a series of excellent properties such as its high specific surface area, outstanding electron transmission property and extraordinary electrocatalytic activity, graphene has been used as a reinforced material for developing high-performance electrochemical sensors or biosensors [11]. For example, Dong's group [12] and Lin's group [13] proved that graphene modified electrodes have a superior electrochemical sensing performance to graphite and single-walled carbon nanotubes.

However, graphene typically suffers from severe aggregation due to the existence of π -stacking interactions and weak van der Waals forces between the graphene sheets, which induce the reduction of the surface area and hinder the transport of electrons [14]. To overcome these defects, conducting polymers, such as polypyrrole (PPY), were deposited on the graphene by the hydrogen bonds and π -stacking interactions between pyrrole molecules and graphene skeletons [15]. This indicated that the PPY/GNs composites improve the electrochemical conductivity beyond that of plain PPY or graphene [16].

Herein, a sensor for the ultrasensitive determination of ATR was presented for the first time based on the PPY–GNs-modified glassy carbon electrode (PPY–GNs/GCE). First, we prepare graphene by using a hydrothermal reduction method. Then, GNs could be used as a template for PPY deposition during the electrochemical polymerization process. The electrochemical behaviors of ATR at the PPY–GNs/GCE, GNs/GCE and bare GCE were investigated. The ATR at the PPY–GNs/GCE had superior electrochemical performance to that at the GNs/GCE and bare GCE. Differential pulse voltammetry (DPV) was used to study the limit of detection and applied to analyze the actual samples, such as tablets, with satisfactory results.

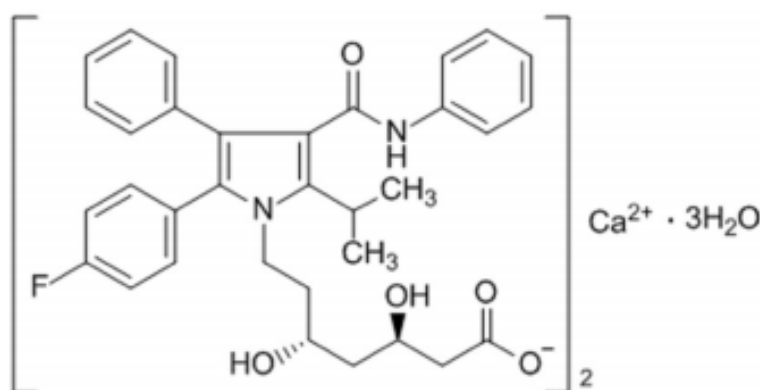


Figure 1. Structure formula of atorvastatin

2. MATERIALS AND METHODS

2.1 Materials

Graphite was obtained from Alfa Aesar. Pyrrole and atorvastatin were purchased from Aladdin and Sigma, respectively. Other chemical reagents were of analytical grade and could be used directly without further treatment.

2.2 Synthesis of PPY-GN composites

Graphite oxide was synthesized from graphite by Hummers' method and was further reduced by a hydrothermal method. Then, the obtained sample was put in a water bath of 60°C for 3h and a stable black dispersion was obtained. The electrolyte solution was formed by mixing pyrrole and sulfuric acid and the solution was subjected to magnetic stirring for 60 min to stabilize the mixture. Meanwhile, a glassy carbon electrode (GCE) was polished to create a mirror surface with alumina suspensions. Afterward, 5 μ L of 0.25 mg/mL GNs was carefully cast on the surface of the well-polished GCE and dried in air. Lastly, PPY-GNs were polymerized potentiostatically from the aforementioned electrolyte solution by applying a potential of 0.5 V for 400 s on GCE. Polymerization was carried out in a common three-electrode system. After the polymerization, the PPY-GNs/GEC was thoroughly washed with ultrapure water and dried prior to the next detection.

2.3 Characterization and apparatus

The microstructures of GNs and PPY/GNs were observed by a scanning electron microscope (Model JSM-7000F, JEOL, Japan). The chemical structure information was investigated using Fourier transform infrared spectrophotometry (FT-IR) (Perkin Elmer Spectrum, PerkinElmer Corp., USA). All electrochemical characterizations and detections, including cyclic voltammetry (CV) and differential pulse voltammetry (DPV) were conducted in a three-electrode setup using a CHI 660D electrochemical workstation (Shanghai Chenhua Limited, China). This three-electrode system in the experiment used the bare and the modified glassy carbon electrode (3 mm in diameter) as the working electrode, respectively. A saturated calomel electrode and a Pt wire electrode were used as the reference and counter electrode, respectively.

3. RESULTS AND DISCUSSION

3.1. Characterization of the CD-GNs

The morphology of GNs and PPY-GNs are presented in Fig. 2. The GNs consisted of large-scale crumpled sheets, while the PPY-GNs showed a three-dimensional network self-supporting structure. It is known from FT-IR (Fig. 3) that a large amount of hydroxyl groups and carbonyl groups exist on the graphene layers, and the abundant nitrogen atoms of polypyrrole in the chain can form

hydrogen bonds with these functional groups on the GN sheets to form a physical cross-linking node. The 3D network of PPY-GNs is formed by the combination of the accumulation of these nodes and the electrostatic repulsion between the graphite sheets. The network structure presents a large number of micron and submicron holes and internal holes are nested inside each other, which provide a transport channel for the electrolyte and increase the contact area between PPY-GNs and atorvastatin, thereby improving the detection sensitivity.

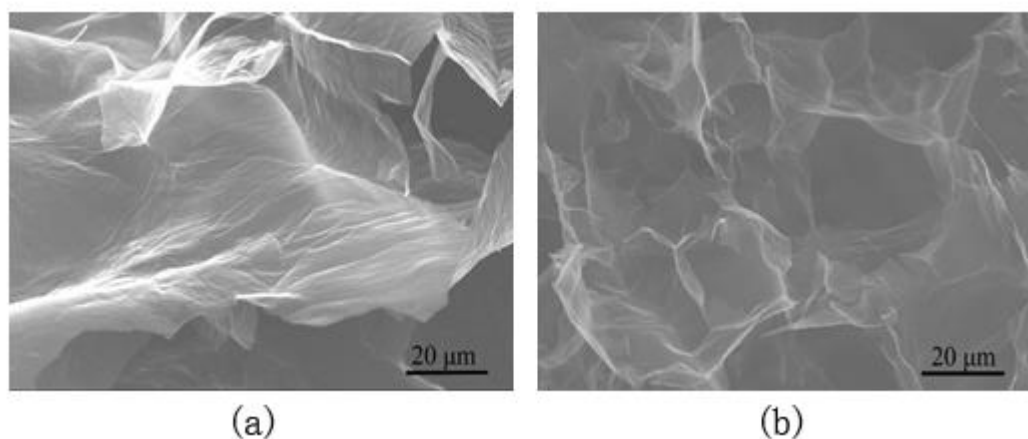


Figure 2. SEM images of (a) GN and (b) PPY-GNs composite

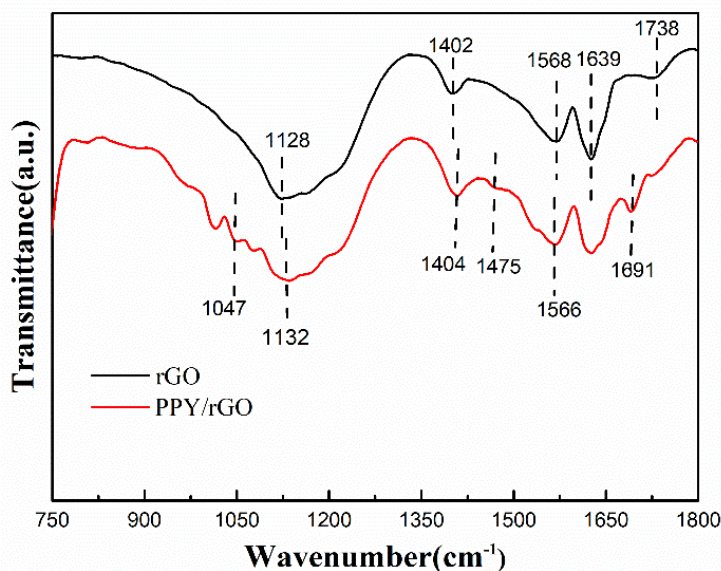


Figure 3. FTIR spectrum of PPY and PPY-GNs composite

To characterize the composite further, the FT-IR spectra of GNs and CD-GNs, shown in Fig. 3, were studied. GNs showed three characteristic peaks at 1738, 1402 and 1128 cm^{-1} , that correspond to the vibration peaks of the C = O stretching in COOH, the C-O stretching in C-OH and C-O-C functional groups, respectively [16,17]. The peak of GNs at 1639 cm^{-1} indicated the vibration of C = C stretching. The peak at 1568 cm^{-1} was mainly due to the vibrations of symmetric stretching of $-\text{CH}_2$

[16,18] It was shown that the GNs has abundant oxygen-containing functional groups and could be used for the in situ adsorption of the pyrrole monomers in the process of polymerization. After chemical polymerization, the peaks at 1404 and 1132 cm^{-1} were derived from the C-OH and C-O-C functional groups of GNs, respectively. The vibration peaks of C = N and C-N stretching of pyrrole ring could be found at 1691 and 1047 cm^{-1} , respectively [19]. The peaks at 1475 cm^{-1} corresponded to the vibration of the NH ring-stretching. The results indicated the successful deposition of PPY on the substrate of GNs.

3.2. Electrochemical behavior of atorvastatin on PPY-GNs/GCE

Requisite cyclic voltammetry (CV) was adopted to evaluate the electrochemical performance of the materials. Fig. 4 compares the CV of 80 μM ATR for bare GCE(a), GNs/GCE(b) and PPY-GNs/GCE(c) in 0.1M phosphate buffer solution. No redox peaks were observed at the bare GCE. A pair of well-defined redox peaks of ATR was observed within the potential window from -0.2 to 0.8 V when the electrode surface is modified by GNs or PPY-GNs, which reveals that ATR underwent a reversible redox process on the electrodes. While at the PPY-GNs/GCE, the peak currents showed a significant increase compared to those observed at the GNs/GCE. The signal enhancement may be attributed to the high conductivity and large specific surface area of PPY-GNs. Furthermore, it was also observed the PPY-GNs composite had smaller values for peak potential (EP) compared with GNs, suggesting that the incorporation of PPY partly enhanced the rate of interfacial electron transmission.

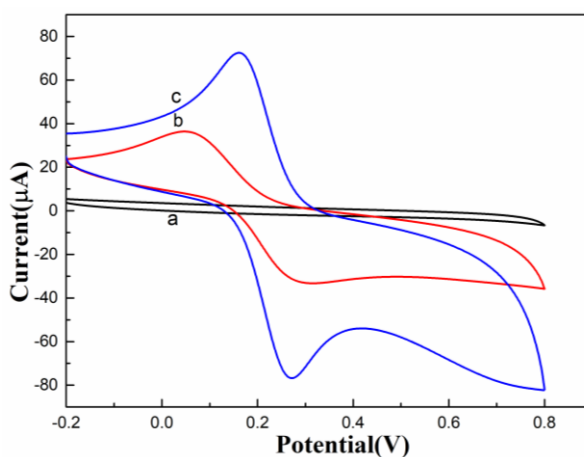


Figure 4. CV of 80 μM atorvastatin at GCE (a), GNs/GCE (b) and PPY-GNs/GCE (c) in 0.1 M phosphate buffer (scan rate: 100 $\text{mV} \cdot \text{s}^{-1}$).

3.3. Effect of solution pH on the oxidation of atorvastatin

The influence of the solution pH on the electrochemical behavior of ATR was studied by CV in the pH range of 3.0~8.0. As shown in Fig. 5a and b, the solution pH affected the peak potentials of ATR. As the pH increased, their peak potentials became negative. These shifts may be ascribed to

participation of protons during the electrode reaction [20]. The linearization equation for the oxidation process was $E_{pa} \text{ (V)} = -0.06 \text{ pH} + 0.4066$ ($R^2=0.98$), where E_{pa} is the peak potential for ATR in V. In addition, the pH had an effect on the peak current. As seen in Fig. 4a, when the pH reaches 4.0, the maximum peak current of ATR appears and then decreased as the pH increased further, which can be due to ATR protonation ($pK_a = 4.46$). The co extraction of OH^- ions at electrode surface interferes ATR response[21]. Therefore, a phosphate buffer with a pH of 4.0 was used as the electrolyte for ATR in all voltammetric determinations.

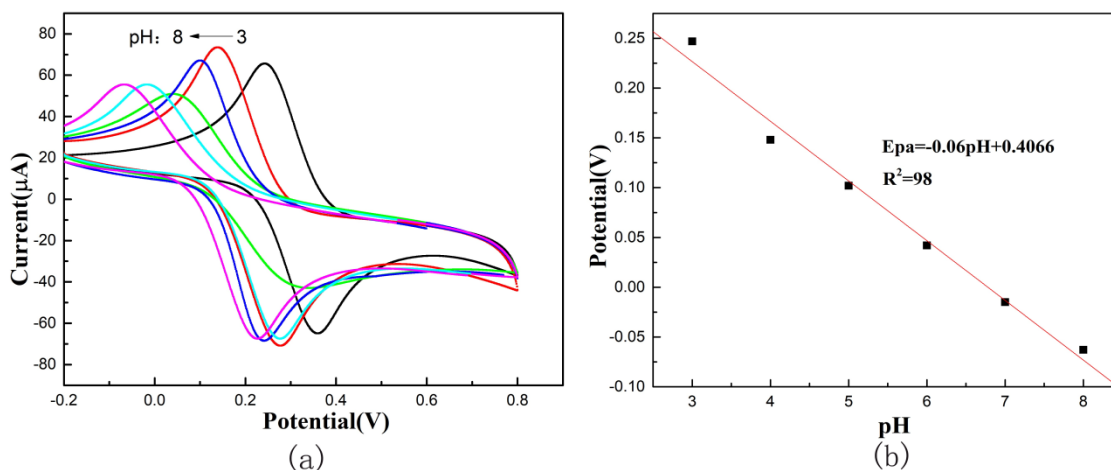


Figure 5. (a) Cyclic voltammograms of PPY-GNs/GCE in PBS containing 80 μM ATR with different pH values in the range of 3.0–8.0 and a scanning rate = 100 mV/s; (b) Plot of E_{pa} vs. pH.

3.4. DPV response of PPY-GNs/GCE for the detection of ATR

Under the above selected conditions, the electrochemical property of PPY-GNs/GCE for ATR detection was investigated by DPV. Figure 6(i) indicates the DPV responses to the varying concentrations of ATR. The peak current of ATR increases linearly with its concentration in the range of 20 μM to 200 μM . The liner equation is $i_p \text{ (}\mu\text{A)} = 13.463 - 1.048C \text{ (}\mu\text{M)}$, where the correlation coefficient is 0.998, i_p is the oxidative peak current in μA and C is the concentration of ATR in μM . The limit of detection (LOD) for ATR is estimated to be 1.191 μM ($S/N=3$) (Fig. 6(ii)). As shown in Table 1, this work is compared with the reported research about detecting ATR. It can be found that the proposed sensor in this work exhibited a broad linear range, which may be ascribed to the synergistic effects of PPY and GNs. Although this work has a higher limit of detection than other methods, such as HPLC and spectrophotometry, the composites are simpler to prepare and easier to control using the in situ polymerization method compared to cetyltrimethyl ammonium bromide at a carbon paste electrode [22].

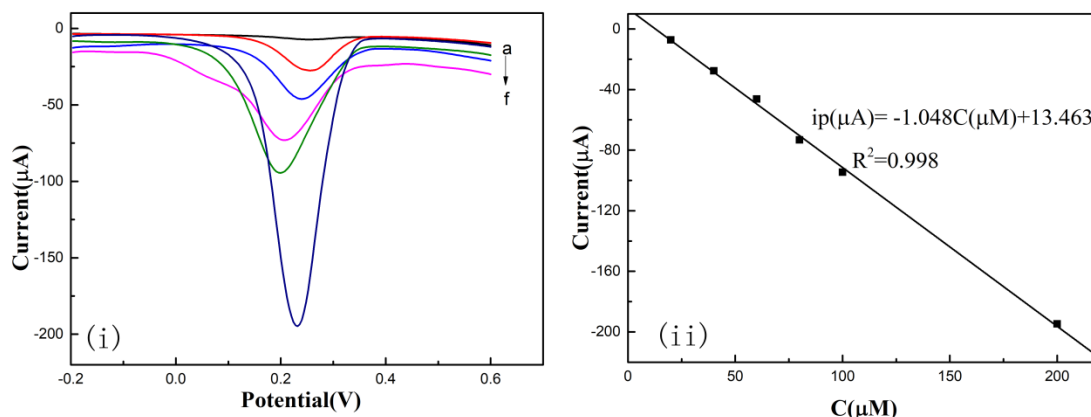


Figure 6. (i) DPV of PPY-GNs/GCE in 0.1 M PBS (pH = 4.0) with different concentrations of ATR: (a) 20, (b) 40, (c) 60, (d) 80, (e) 100 and (f) 200 μM; (ii): plot of the peak current vs. the concentration of ATR.

Table 1. Comparison of the proposed method with some of the reported determinations of ATR

Method	Type of electrode	Linear concentration range (μg/mL)	Detection limit (μg/mL)	References
HPLC	-	0.50-86.0	0.0084	[2]
Spectrophotometry	-	5.00-25.0	1.0700	[5]
Voltammetry	CTAB-CPE	0.027-5.58	0.0022	[22]
Voltammetry	GCE	2.41-120	0.7195	[23]
Voltammetry	PPY-GNs/GCE	24-240(20~200 μM)	2.292(1.191 μM)	This work

3.5. Tablet sample analysis

The modified GCE was also applied to the differential pulse voltammetric analysis of ATR in its tablets (20 and 40 mg per tablet). In addition, the recovery studies were performed. As shown in Table 2, the recoveries were found to be in the range of 98.6 – 99.2%. The good recoveries of the samples suggest that this method is well suited for application to the detection of atorvastatin in tablet samples.

Table 2. The determination of ATR from tablets.

Sample	Labeled (mg/tablet)	Found (mg/tablet)	Recovery%
ATR tablet	10	9.86	98.6
	20	19.84	99.2

4. CONCLUSIONS

In summary, a facile and reinforced electrochemical sensor based on PPY–GNs was developed for the detection of atorvastatin by a differential pulse voltammetric method. The PPY-GNs composite showed a 3D porous architecture with a large specific surface area. It was found that the incorporation of PPY-GNs sheets not only enlarged the effective area of the composite but also improved the rate of interfacial electron transfer. The PPY–GNs/GCE with high sensitivity and a broad linear range provide a convenient candidate for the trace analysis of ATR in tablet samples.

ACKNOWLEDGEMENTS

The authors are thankful for the financial support provided by the Science and Technology Research Project of Yuncheng University, China (CY-2017009).

References

1. B.W. McCrindle, L. Ose, A.D. Marais, *J. Pediat.*, 143 (2003) 74.
2. T.G. Altuntas, N. Erk, *J. Liq. Chromatogr. Relat. Technol.*, 27 (2004) 83.
3. P. Rukthong, P. Sangvanich, S. Kitchaiya, E. Jantratid, K. Sathirakul, *J. Sci. Technol.*, 35 (2013) 41.
4. W.W. Bullen, R.A. Miller, R.N. Hayes, *J. Am. Soc. Mass Spectrom.*, 10 (1999) 55.
5. M. Hasan, Z. Ahmed, M.R. Amin, N.S. Sherin, *Int. J. Pharm. Res. Dev.*, 2 (2011) 116.
6. Y.Z. Baghdady, M.A. Al-Ghobashy, A.A.E. Abdel-Aleem, S.A. Weshahy, *J. Adv. Res.*, 4 (2013) 51.
7. S. Bernard, M. Mathew, *J. Appl. Pharm. Sci.*, 2 (2012) 150.
8. S.F. Rassi, *Anal. Chem. Res.*, 12 (2017) 65.
9. F. Jalali, M. Ardeshiri, *Mater. Sci. Eng., C*, 69 (2016) 276.
10. K.S. Novoselov, A.K. Geim, S.V. Morozov, D. Jiang, Y. Zhang, S.V. Dubonos, I.V. Grigorieva, A.A. Firsov, *Science*, 306 (2004) 666.
11. D. Chen, L. Tang, J. Li, *Chem. Soc. Rev.*, 39 (2010) 3157.
12. M. Zhou, Y. Zhai, S. Dong, *Anal. Chem.*, 81 (2009) 5603.
13. D. Du, Z. Zou, Y. Shin, J. Wang, H. Wu, M.H. Engelhard, J. Liu, I.A. Aksay, Y. Lin, *Anal. Chem.*, 82 (2010) 2989.
14. C. Xu, J. Sun, L. Gao, *J. Mater. Chem.*, 21 (2011) 11253.
15. M. Deng, X. Yang, M. Silke, W. Qiu, M. Xu, G. Borghs, H. Chen, *Sens. Actuators, B*, 158 (2011) 176.
16. C. Bora, SK. Dolui, *Polymer*, 53 (2012) 923.
17. H. Han, H. Lee, J. You, H. Jeong, S. Jeon, *Sens. Actuators, B*, 190 (2014) 886.
18. M. Deng, X. Yang, M. Silke, W. Qiu, M. Xu, G. Borghs, H. Chen, *Sens. Actuators, B*, 158 (2011) 176.
19. L. Chen, X. Guo, B. Guo, S. Cheng, F. Wang, *J. Electroanal. Chem.*, 760 (2016) 105.
20. D.B. Shikandar, N.P. Shetti, R. M. Kulkarni, *Sens. Actuators, B*, 255 (2018) 1462.
21. S.D. Bukkitgar, N.P. Shetti, *ChemistrySelect*, 1 (2016) 771.
22. J.C. Abbar, S.T. Nandibewoor, *Colloids Surf., B*, 106 (2013) 158.
23. G. Férey, *Chem. Soc. Rev.*, 37 (2008) 191.